Acquisition Performance of Galileo E5a Signal

Youssef Tawk, Cyril Botteron, Aleksandar Jovanovic, Pierre-André Farine
Ecole Polytechnique Fédérale de Lausanne, Institute of Microengineering (IMT)
Electronics and Signal Processing Laboratory, Breguet 2, 2000 Neuchâtel, Switzerland

***Abstract*—The introduction of new modulations on the global navigation satellite systems brings potential improvements for ground positioning. Clever receiver designs taking advantage of the characteristics of the new signals will be able to achieve better accuracy, higher sensitivity, improved multipath mitigation and tracking robustness. In this context, this paper focuses on the Galileo E5a signal and study different acquisition architectures that can be applied on this signal. Their performances are discussed in terms of detection sensitivity and by a theoretical characterization of the false alarm and detection probabilities. The theoretical results are validated by measurements using a Spirent constellation simulator, a Fraunhofer triple band front-end and a non real time software receiver.**

I. Introduction

The modernized GNSS signals present great advantages for user ground receivers in improving their performances. The new modulations like BOC (Binary Offset Carrier), CBOC (Composite BOC) and AltBOC (Alternative BOC) have a great potential for multipath mitigation. The new tiered code structure improves the correlation proprieties and the new Data/Pilot signals allows longer integration time and hence improved sensitivity. However, all these new innovations present new challenges for designers to implement receivers which make use of these new characteristics. In the past there have been several works targeting new architectures for acquiring and tracking these signals. In [1], F. Bastide et al. analyzed the acquisition and tracking of the L5/E5 signals. In [2], N. Shivaramaiah et al. discussed the possibilities of acquiring Galileo E5 signal. In [3], V. Heiries et al. analyzed and compared the acquisition performance for BOC signals.
In this paper, the focus is on the acquisition of the BPSK(10) Galileo E5a signal. Different acquisition strategies are presented such as coherent and non coherent integration of pilot and/or data channels. The performances of these methods are presented in terms of theoretical evaluation of the probability of detection and probability of false alarm. Furthermore, these results are supported by practical measurements using a receiver platform composed of a Spirent simulator, a Fraunhofer triple band front-end, and a non-real time software receiver to post process the signal.

This paper is divided as follows: in section II, the structure of the Galileo E5a signal is presented. In section III, the architecture of the acquisition process is discussed and the performances of different strategies are presented. In section IV and V, simulation and experimental results are shown and finally the conclusions are provided in section VI.

II. Signal Structure

The new transmitted Galileo E5a signal can be extracted from the general E5 AltBOC signal [4] and approximated at the input of the receiver as:

$$r_{E5a}(t) = \sum_{i=1}^{N} A_i e_{E5ai}(t-\tau) e^{j(2\pi(f_c+f_{0i})t+\phi_{0i})} + \beta(t) \quad (1)$$

where N is the number of satellites, A_i is the amplitude of the i^{th} satellite, f_c is the carrier frequency equal to 1176.45 MHz, f_0 is the Doppler frequency, ϕ_0 is the phase offset introduced by the transmission channel, τ is the code delay and β is the noise in the channel which is assumed to be white Gaussian distributed. e_{E5ai}, the spreading code carried on the E5a band, contains the data and pilot channels and is equal to:

$$e_{E5a}(t) = d_{E5aI}(t) c_{E5aI}(t) s_{E5aI}(t) + j(c_{E5aQ}(t) s_{E5aQ}(t)) \quad (2)$$

where c_{E5aI} and c_{E5aQ} are the primary codes on each channel, s_{E5aI} and s_{E5aQ} the secondary codes, and d_{E5aI} is the data message. Table I summarizes the characteristics of the E5a signal. Hereafter, for the sake of clarity, only one satellite is considered. After down converting and digitizing the signal, the output of the front end can be expressed as:

Channel	Code length [chips]		Code length [ms]	Symbol Rate
	Primary	Secondary		
E5a-I	10230	20	20	50
E5a-Q	10230	100	100	No data

TABLE I
E5a Signal Characteristics

$$r_{IF}(nT_s) = A e_{E5a}(nT_s - \tau) e^{j(2\pi(f_{IF}+f_{0i})nT_s+\phi_{0i})} + \beta(nT_s) \quad (3)$$

where f_{IF} is the intermediate frequency after down conversion and T_s the sampling period. r_{IF} is then sent to the post processing stage, where the acquisition, tracking, pseudoranges and data bits extraction are performed.

III. Acquisition Architectures

The job of the acquisition block in a receiver is to detect the presence of a satellite. The detection is performed by transforming the signal at the intermediate frequency into a baseband signal and then multiplying it by a locally generated PRN code. After integration and dump, a threshold is set, and if the correlation peak passes this threshold, the corresponding satellite is considered as available. Thus the signal acquisition

consists in a two dimensional search distributed among code phase and Doppler frequency. Different acquisition techniques exist, e.g. serial acquisition, parallel frequency space acquisition and parallel code space acquisition [6]. In this paper, the last method is considered as it has the fastest computation time. Figure 1 shows the general acquisition block for the E5a signal. The PRN code generator can generate simultaneously

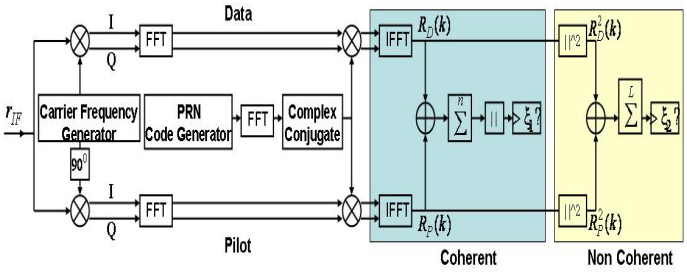

Fig. 1. General Acquisition Architecture for Galileo E5a based on the parallel code space acquisition

or separately the pilot and data PRN codes, depending if a data and/or pilot are required. This combination allows to have five acquisition strategies that can be applied on E5a:

S1: Coherent integration of data or pilot channels
S2: Coherent integration of data and pilot channels
S3: Coherent integration of data and pilot channels during 'n' primary code periods and non-coherent combining of 'L' integrations
S4: Non-Coherent integration of data or pilot channels
S5: Non-Coherent integration of data and pilot channels

To compare these strategies, two points should be taken in consideration: sensitivity and probability of detection. In coherent integration, the squaring is performed after the summation and the CDMA processing gain is equal to $10log(n)$, where n is the number of primary code periods. In non coherent integration, the squaring is performed before the summation, which will lead to a non coherent loss that can be expressed in dB as [5]:

$$L(n) = 10log\left(\frac{1+\sqrt{1+0.438n}}{2.2}\right) \tag{4}$$

The non-coherent gain will then be equal to the coherent gain minus the non-coherent loss. The difference between the two gains for different integration periods is shown in Figure 2. When acquiring coherently data and pilot together, a 3 dB additional gain is achieved as in each ms there is a combination of two uncorrelated signals that have equal power. If the two channels are acquired non-coherently a 2.68 dB additional gain is added. A coherent combining therefore has a better gain than its non-coherent counterpart and hence a better sensitivity can be achieved. The draw-back in coherent integration remains in the existence of bit sign ambiguity resulting from the data bits on the data channels and from the secondary code chips on both data and pilot channels. As the receiver has no prior information about the data bit and secondary bit signs, the addition of the correlation of consecutive primary code periods

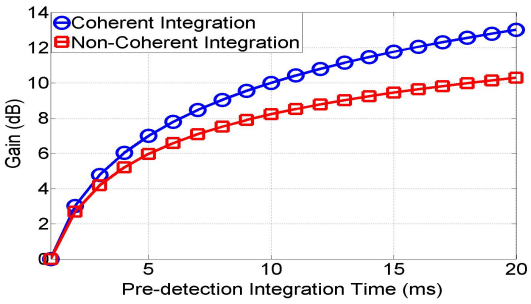

Fig. 2. Coherent versus non-coherent gain assuming no data bit transition during the integration time

can results in energy loss if the bit transition exists in the integration period. This issue can be solved using non-coherent integration by squaring the correlation results before adding. In this case no different correlation signs can cancel each other and no power is lost. An additional advantage for non-coherent integration is that a smaller number of operations is required which leads to a faster acquisition.

Another criterion needed for comparison is the computation of the probability of detection and false alarm. The strategies resulting in the same output combination (i.e. coherent or non-coherent), their responses will have a similar statistical distribution and hence S1 and S2 can be categorized as coherent combining and S3, S4 and S5 as non-coherent combining. In the following, the probability of detection and false alarm are evaluated for these two categories for the general case of data and pilot combining. In the case of data or pilot only, the computations can be derived from the equations below and hence only simulation results are presented after.

A. Coherent Combining

The signal detection problem is set up as a hypothesis test, testing the hypothesis that the signal is present versus the hypothesis that the signal is not present. The test statistic for the derivations in the case of coherent combining at the k_{th} output correlator is defined as follows:

$$S_k = \left|\sum_{i=1}^{nM}\left(R_{Di}(k) + R_{Pi}(k)\right)\right| \tag{5}$$

where M is the number of primary code chips summed prior to squaring and n the number of coherent integration. R_D and R_P are the correlators output of the data and pilot channels and can be expressed as:

$$R_D(k) = R_{DI}(k) + jR_{DQ}(k) \tag{6}$$

$$R_P(k) = R_{PI}(k) + jR_{PQ}(k) \tag{7}$$

where I and Q are the in phase and quadrature components of each branch. Replacing (6) and (7) in (5), the final decision is expressed as:

$$S_k = \sqrt{\sum_{i=1}^{nM}\left(R_{DIi}(k) + R_{PIi}(k)\right)^2 + \left(R_{DQi}(k) + R_{PQi}(k)\right)^2} \tag{8}$$

To find the threshold and the probability of detection for S_k, the nature of its distribution and the probability density function should be known. Assuming the noise at the input of the correlators is zero mean Gaussian distributed with variance σ^2, then according to the central limit theorem (CLT), if nM is sufficiently long, the noise at the output of the Fast Fourier Transform (FFT) correlators is zero mean Gaussian distributed with variance $cnM\sigma^2$ where $c = 2$ in case of data and pilot combining, and $c = 1$ in case of data or pilot only. In the absence of signal, the magnitude of S_k is Rayleigh distributed and the probability of false alarm is the probability that one or more correlators output is greater than the threshold. It can be written as [6]:

$$p_{fa} = 1 - (1 - e^{-\frac{TH^2}{2cnM\sigma^2}})^N \tag{9}$$

where N is the number of padded FFT. With the presence of a signal at the k^{th} output, S_k is Rician distributed. The probability that an output is higher than a given threshold TH is given by [6]:

$$p\left(S_k \geq TH\right) = Q\left(\frac{S_k}{\sqrt{cnM\sigma^2}}, \frac{TH}{\sqrt{cnM\sigma^2}}\right) \tag{10}$$

Where Q denotes the Markum Q function. Finally, as a signal will be detected if one or more FFT bins output is greater than the threshold, the probability of detection can be computed as:

$$p_d = 1 - \prod_{k=1}^{N}\left(1 - Q\left(\frac{S_k}{\sqrt{cnM\sigma^2}}, \frac{TH}{\sqrt{cnM\sigma^2}}\right)\right) \tag{11}$$

B. Non-Coherent Combining

In the case of non-coherent combining, the test statistic at the k^{th} output correlator is defined as:

$$S_k = \sum_{j=1}^{L}\left(\sum_{i=1}^{nM}\left(|R_{Di}(k)|_j^2 + |R_{Pi}(k)|_j^2\right)\right) \tag{12}$$

where L is the number of non-coherent integrations. If there is no signal at the input of the correlators, and the noise is zero mean Gaussian distributed with variance σ^2, then according to the CLT, the outputs of the FFT correlators will a have random Gaussian distribution with zero mean, variance $cnM\sigma^2$ and $|R_{Di}(k)|$ and $|R_{Pi}(k)|$ will have a Rayleigh distribution. The sum of N Rayleigh^2 distribution variables of variances σ^2 is a gamma distribution with parameters N and $2\sigma^2$ [7]. Hence, in the case of non-coherent combining of data and pilot channels of E5a, S_k will have a Gamma distribution with parameters cL and $cnM\sigma^2$. The probability of false alarm is the probability of one or more correlator outputs are greater then a given threshold. It is equal to [7]:

$$p_{fa} = 1-(1-p(S_k \geq TH))^N = 1-\left(\frac{\gamma(cL, TH/cnM\sigma^2)}{\Gamma(cL)}\right)^N \tag{13}$$

where $\gamma()$ is the lower incomplete Gamma function [7]. If the signal is present, then the inphase and quadrature outputs are statistically independent and identically distributed Gaussian random variables with means $m_{DI}(k)$, $m_{PI}(k)$, $m_{DQ}(k)$, and $m_{PQ}(k)$ and the same variance $nM\sigma^2$. The sum of the squares for L non coherent integration (i.e. S_K) will have then a non central chi square distribution, with 2cL degrees of freedom and a non centrality parameter as:

$$\lambda_k^2 = \sum_{i=1}^{L}\left(m_{DIi}^2(k) + m_{PIi}^2(k) + m_{DQi}^2(k) + m_{PQi}^2(k)\right) \tag{14}$$

The probability that an output is higher than a given threshold TH is given by:

$$p\left(S_k \geq TH\right) = Q_{cL}\left(\sqrt{\frac{\lambda_k^2}{cnM\sigma^2}}, \sqrt{\frac{TH}{cnM\sigma^2}}\right) \tag{15}$$

where $Q_n(\alpha, \beta)$ is the generalized Marcum-Q function. Finally the probability of detection can be computed as:

$$p_d = 1 - \prod_{k=1}^{N}\left(1 - Q_{cL}\left(\sqrt{\frac{\lambda_k^2}{cnM\sigma^2}}, \sqrt{\frac{TH}{cnM\sigma^2}}\right)\right) \tag{16}$$

IV. Simulation Results

In order to compare the performance for different acquisition architectures, P_{fa} has to be fixed and the corresponding TH has to be calculated to reach this value. In the case of coherent integration, Figure 3 shows P_{fa} as a function of TH for different numbers of padded FFT. It is clear that increasing the FFT size or decreasing TH results in an increase of P_{fa}. Once a P_{fa} is fixed and N is chosen, TH can be derived and P_d can be obtained. In Figure 4, P_d for a 3 ms

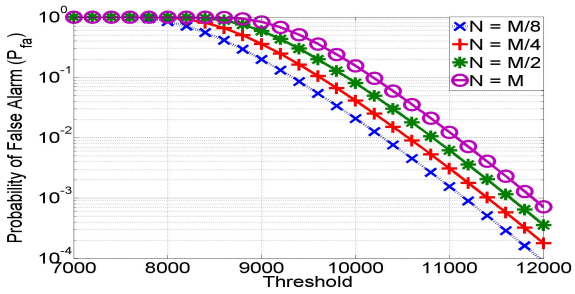

Fig. 3. Probability of false alarm for different output correlators for coherent integration

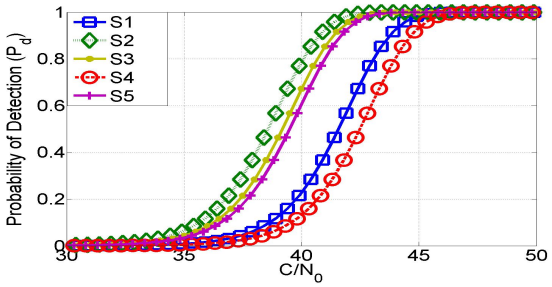

Fig. 4. Probability of detection for a 3 ms integration time for the 5 strategies mentioned in section III assuming a $P_{fa} = 1e-5$

integration period for the five strategies mentioned in section III are shown when N=M, assuming a P_{fa}=1e-5. We can see that coherent integration of data and pilot channels during one primary code period and non-coherent combining over the whole integration length (S3) has a close performance to non-coherent integration of both channels (S5) as the non-coherent loss is considered only during one primary code period. In

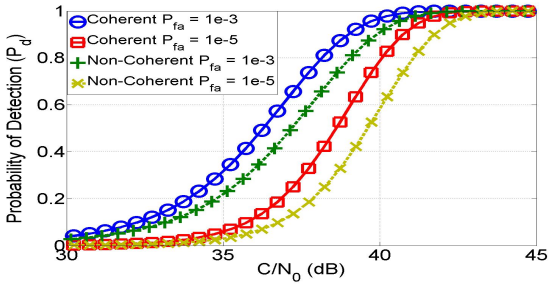

Fig. 5. Comparison between Probability of detection for a 3 ms coherent and non-coherent integration of data and pilot channels

Figure 5, P_d's for S2 and S5 are shown for different P_{fa}. It is clear that when P_{fa} is higher P_d is higher. Also in coherent combining P_d is better than in non-coherent combining due to the higher sensitivity and less noisy response.

V. Experimental Results

In order to validate the theoretical results obtained, a receiver platform for acquiring the E5a signal has been built. A Spirent GSS8000 simulator [8] is used to generate the E5 signal. The created scenario consists of having two satellites vehicles copied in the same position, one with a fixed high power for reference measurements, and the other with a varying power. The signal generated is downconverted and digitized by a triple band L1, L2 and L5 (E5a) Fraunhofer front-end. For the baseband processing, a Matlab based acquisition receiver has been built to test different architectures. The frequency step used to search the frequency space is 0.25 kHz, and the code step is 0.25 chips. Experimental results were obtained by averaging 100 simulations for each C/N_0 and calculating the number of times the receiver detects the signal. In Figure 6, a comparison between theoretical and experimental results for a 1 ms coherent combining of data and pilot channels is shown and in Figure 7 the comparison is made for a 3 ms non coherent combining. In both cases, it can be seen that a good match between theoretical and experimental results are obtained. In the case of coherent combining for more then 1 ms, the computational load is very high as an exhaustive search of all the combination of the secondary code bits have to be computed. This issue can be solved with non-coherent combining as the sign ambiguity is resolved by squaring and hence the computational load is decreased.

VI. Conclusion

This paper discussed different acquisition strategies for Galileo E5a. Theoretical expressions for false alarm and

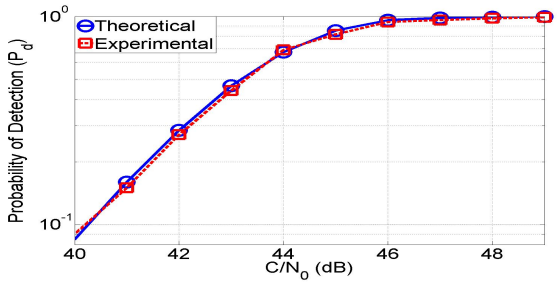

Fig. 6. Theoretical and experimental results for a 1 ms coherent integration of data and pilot assuming a P_{fa} =1e-5

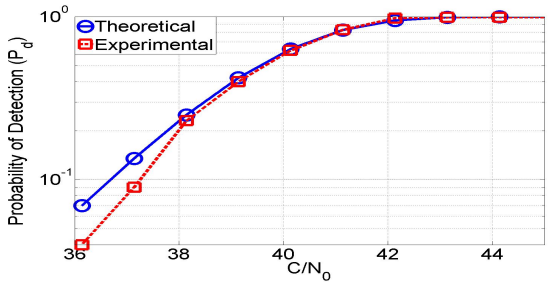

Fig. 7. Theoretical and experimental results for a 3 ms non-coherent integration of data and pilot assuming a P_{fa} =1e-5

detection probability for coherent and non-coherent combining of data and pilot channels were computed. It was shown that coherent combining performs better with respect to sensitivity and detection probability but non-coherent combining is better to deal with data bit ambiguity and has a lower computational load. Finally a full configuration setup was build to acquire E5a and experimental results were derived to support the theoretical ones.

VII. Acknowledgment

The authors are grateful for the financial support from the Swiss National Science Foundation (http://www.snf.ch/) who supports this work under grant 200021120187/1.

References

[1] F. Bastide, O. Julien, C. Macabiau, and B. Roturier, *'Analysis of L5/E5 acquisition, tracking and data demodulation threshold'*, ION GPS/GNSS, Portland, OR, Sept. 2002, pp. 2196 2207.

[2] N.C.Shivaramaiah, A.G.Dempster, 'Galileo E5 signal acquisition strategies', Coordinates Magazine, IV(8), 12-16, August 2008.

[3] V. Heiries, D. Roviras, L. Ries, V. Calmettes, 'Analysis of Non Ambiguous BOC Signal Acquisition performance', ION GNSS 17th International Technical Meeting of the Satellite Division, 21-24 Sept. 2004, pp. 26112622.

[4] Galileo Joint Undertaking, 'Galileo Open Service Signal In Space Interface Control Document', Draft 1, February, 2008

[5] J. Bao, Y. Tsuo, 'Fundamentals of Global Positioning System Receivers', John Wiley and Sons, Hoboken, New Jersey 2005.

[6] C. Botteron, G. Walchli, G. Zamuner, M. Frei, D. Manetti, F. Chastellain, P.-A. Farine, P.Brault, 'A flexible Galileo E1 Receiver Platform for the Validation of Low Power and Rapid Acquisition Schemes', ION GNSS Forth Worth 2006.

[7] Sijbers J, Poot D, den Dekker AJ, Pintjens W, Automatic estimation of the noise variance from the histogram of a magnetic resonance image, Physics in Medicine and Biology, Vol. 52, Nr. 5, p. 1335-1348, (2007)

[8] http://www.spirent.com/Solutions-Directory/GSS8000.aspx